Nonisentropic Potential Formulation for Transonic Flows

Goetz H. Klopfer* and David Nixon†
Nielsen Engineering & Research, Inc., Mountain View, California

A potential equation for nonisentropic transonic flows is formulated. This procedure captures shock waves with Rankine-Hugoniot strengths, but retains the simplicity of the traditional potential equation. Numerical computations are presented that verify the efficiency of the present procedure. It is also shown that Crocco's theorem is not applicable to potential flows. A new Crocco's theorem valid for potential flows is derived and it is shown that transonic flows with nonconstant shock strengths can never be irrotational, irrespective of whether the flow is isentropic or not.

I. Introduction

THERE are many ways of formulating the full potential equations for transonic flows. Each has its own degree of accuracy and ease of application. The traditional formulation is based on the integrated energy equation, mass conservation, and isentropicity. However, this formulation is motivated mainly by mathematical convenience and is not necessarily physically accurate. For example, we may wish to conserve the streamwise momentum instead of mass—or we may wish to allow for entropy changes. We will briefly look at the various formulations to arrive at some conclusion regarding accuracy (in the physical sense) and ease of application (in the numerical sense).

In the usual derivation of the potential formulation, the relation between the normal entropy gradient and vorticity, first derived by Crocco,[1,2] is used. Crocco's theorem shows that, in an inviscid flow with constant total enthalpy, the vorticity produced is an explicit function of the entropy gradient normal to the streamlines. If there are no shock waves in an inviscid flow with uniform reservoir conditions, then the flow is isentropic, which makes the entropy gradient and hence the vorticity zero everywhere. This is a special case of flows with zero normal entropy gradient. In this study, we investigate some of the properties of potential flows that contain discontinuities.

In the following sections we will look into the various formulations of the one-dimensional steady potential equations (Sec. II) when shock waves are present in the flow. In Sec. III we investigate the connection between vorticity and entropy. A formulation of the potential equation that is not isentropic is presented in Sec. IV. Some numerical results are given in Sec. V.

II. Potential Equations

In this section the various possible formulations of the full potential equations are investigated (see also Ref. 3). Attention will be limited to steady one-dimensional flows, although to compare the relative merits of the various formulations higher dimensions need to be considered.

The governing equations considered are the Euler equations representing conservation of mass, momentum, and energy. Consider the discontinuity surface shown in the sketch of Fig. 1. States upstream of the surface are denoted by subscript *1* and downstream by subscript *2*. It is clear that only shock waves are possible for steady flows; the contact surface must degenerate into the case where the flow properties are identical on both sides of the surface. The states 1 and 2 are given by the jump relations of the Euler equations

$$[\rho u]=0, \qquad [\rho u^2+p]=0, \qquad [(e+p)u]=0 \tag{1}$$

where $[f]\equiv f_2-f_1$, pressure $p=(\gamma-1)[e-(u^2/2)]$, ρ is the density, u the velocity, the total energy $e=\rho[i+(u^2/2)]$, i is the specific internal energy, and γ the ratio of specific heats.

The last relation of Eq. (1) can be rewritten in terms of total enthalpy, $h_0=(e+p)/\rho$, as

$$[\rho u h_0]=0 \tag{2}$$

which gives $h_0=\text{const}$.

The pressure and density ratio for the Euler jumps (also known as the Rankine-Hugoniot relations) are given in terms of the upstream Mach number by

$$\frac{p_2}{p_1}=\frac{2\gamma M_1^2-(\gamma-1)}{\gamma+1} \tag{3}$$

$$\frac{\rho_2}{\rho_1}=\frac{(\gamma+1)M_1^2}{2+(\gamma-1)M_1^2} \tag{4}$$

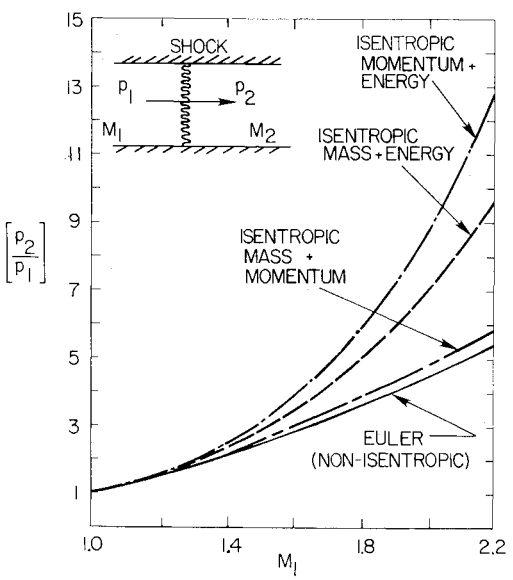

Fig. 1 Pressure ratio across a one-dimensional shock for various approximations.

Presented as Paper 83-0375 at the AIAA 21st Aerospace Sciences Meeting, Reno, Nev., Jan. 10-13, 1983; received Feb. 1, 1983; revision received Aug. 29, 1983.

*Research Scientist. Member AIAA.

†Manager, Computational Fluid Dynamics Department. Associate Fellow AIAA.

Similar expressions can be obtained for the velocity and energy ratios. With these jump conditions for the flow variables, mass, momentum, and energy are conserved across the discontinuity surface. The entropy change across the surface is

$$\exp\left(\frac{s_2-s_1}{c_v}\right)=\frac{(p_2/p_1)}{(\rho_2/\rho_1)^{\gamma}} \tag{5}$$

where c_v = specific heat at constant volume. From the second law of thermodynamics

$$s_2-s_1\geq 0$$

Therefore, Eqs. (3-5) show that the upstream Mach number must be either sonic or supersonic for a discontinuity to exist. And if jump is to be isentropic, then $M_1\equiv 1$, for which case $p_2=p_1$ and $\rho_2=\rho_1$, that is, a jump of zero strength.

While it is usual for the potential approximations of the equations to assume that the flow is isentropic, the above derivation of the jump conditions shows that it is not possible to satisfy all of the conservation equations unless the jump is of zero strength. If the shocks are of nonzero strength, then the addition of the isentropic relation makes the system of equations overdetermined and consequently one of the three conservation equations must be dropped in order to obtain a properly posed problem. Each of the three possibilities will be discussed.

Mass-Momentum Conservation

In this potential formulation, mass and momentum are conserved and energy is not conserved across a shock wave. The pressure ratio is given implicitly by

$$M_1^2=\frac{1}{\gamma}\left[\frac{(p_2/p_1)-1}{1-(p_2/p_1)^{-1/\gamma}}\right] \tag{6}$$

An energy deficit can be defined as

$$\frac{\Delta h_0}{h_{01}}=\frac{h_{01}-h_{02}}{h_{01}}$$
$$=\frac{1+[(\gamma-1)/2]M_1^2[1-(p_2/p_1)^{-2/\gamma}]-(p_2/p_1)^{(\gamma-1)/\gamma}}{1+[(\gamma-1)/2]M_1^2} \tag{7}$$

where M_1^2 is given by Eq. (6) in terms of the pressure ratio across the shock wave. The energy deficit represents the loss of energy conservation due to the isentropic flow assumption.

Mass-Energy Conservation

Here the mass and energy are conserved and momentum is not. This is the traditional potential formulation. For this formulation, the pressure ratio across a shock wave is

$$M_1^2=\frac{2}{\gamma-1}\left[\frac{(p_2/p_1)^{(\gamma+1)/\gamma}-(p_2/p_1)^{2/\gamma}}{(p_2/p_1)^{2/\gamma}-1}\right] \tag{8}$$

The loss of momentum conservation is given by

$$\frac{\Delta(\rho u^2+p)}{(\rho u^2+p)_1}=\frac{1+\gamma M_1^2[1-(p_2/p_1)^{-1/\gamma}]-(p_2/p_1)}{1+\gamma M_1^2} \tag{9}$$

where M_1^2 is given by Eq. (8) in terms of p_2/p_1.

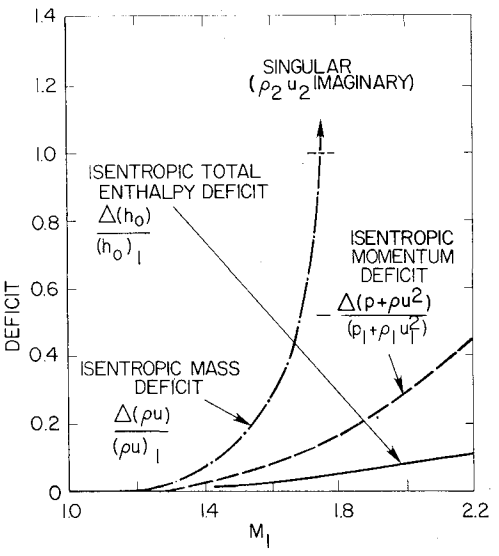

Fig. 2 Energy, momentum, and mass deficit across a one-dimensional isentropic shock for various approximations.

Momentum-Energy Conservation

The pressure ratio across a shock wave is given by

$$M_1^2=\frac{1+(\gamma+1)/(\gamma-1)\,(p_2/p_1)-[2\gamma/(\gamma-1)]\,(p_2/p_1)^{1/\gamma}}{\gamma[(p_2/p_1)^{1/\gamma}-1]} \tag{10}$$

The mass deficit is given by

$$\frac{\Delta(\rho u)}{(\rho u)_1}=1-\left\{\left(\frac{p_2}{p_1}\right)^{1/\gamma}\left[\frac{1+\gamma M_1^2-(p_2/p_1)}{\gamma M_1^2}\right]\right\}^{1/2} \tag{11}$$

where M_1^2 is given by Eq. (10).

The pressure ratios and conservation deficits are shown in Figs. 1 and 2 for the various formulations. Also included is the Euler or Rankine-Hugoniot pressure jump. As can be seen, the isentropic potential formulation that agrees best with the Euler results is the one that conserves both mass and momentum but not energy. This is indicated by the pressure ratio (almost Eulerian) and the energy deficit. The formulation with the worst agreement is the isentropic conservation of momentum and energy. For upstream Mach numbers greater than 1.2, the pressure ratio rapidly diverges from the Eulerian pressure ratio. The deficit (mass flux for this formulation) shows an even bleaker picture. The mass deficit becomes singular at about $M_1=1.74$; beyond this point the downstream mass flux is imaginary [see Eq. (11)]. Thus, this formulation is not valid (i.e., the flow is nonphysical) for local Mach number beyond 1.74 and probably is well below this limit. It should be noted that for transonic flows the shock will induce flow separation at a local Mach number of about 1.3, thus invalidating the inviscid assumption of the Euler equations. However, even at this upstream Mach number, the error introduced by the isentropic assumption is significant.

The traditional potential formulation, isentropic conservation of mass and energy, is between the other two formulations. It is somewhat better than isentropic mass and momentum conservation. It is clear from Figs. 1 and 2 that if isentropicity is enforced, then the order of importance of the violation of the conservation equations is mass, momentum, and energy.

The above ordering is based on physical arguments only, that is, which formulation represents best the Eulerian

equations of gasdynamics. However, as often is the case, mathematical convenience and expediency overwhelm physical accuracy for the potential equations. From a mathematical standpoint, the ordering is quite different—it is energy and mass, energy and momentum, and, finally, mass and momentum conservation for isentropic flow. The reason for this is twofold. First, both the energy and mass equations are scalar differential equations. Thus, any potential formulation based on these two equations extends immediately to two- or three-dimensional flows. The second reason is that the energy equation can be integrated to give

$$h_0 = \text{const} \tag{12}$$

along a streamline (steady flows only). If the upstream reservoir conditions are uniform, which is the usual case for external transonic flows, then the total enthalpy is constant everywhere. Thus, for the traditional potential formulation, the problem reduces to the solution of only one differential equation rather than the system of equations that result from alternative formulations.

Another type of formulation that is possible and has not been discussed so far is one based on nonisentropic flows. In other words, we do not make the isentropic assumption. Equation (5) gives the entropy rise through a Rankine-Hugoniot shock wave. This is also shown in Fig. 3. Now consider an approximation based on the nonisentropic conservation of mass and energy together with an equation of the form $p/p^\gamma = K(S)$, a function of entropy. In this case the pressure ratio across a shock wave is given by

$$M_1^2 = \frac{2}{\gamma-1}\left[1-K^{1/\gamma}\left(\frac{p_2}{p_1}\right)^{(\gamma-1)/\gamma}\right]\Big/\left[K^{2/\gamma}\left(\frac{p_2}{p_1}\right)^{-2/\gamma}-1\right] \tag{13}$$

where $K = \exp[(s_2 - s_1)/c_v]$.

In general, an arbitrarily specified form of $K(S)$ in this formulation will lead to a solution that does not conserve momentum. However, if the flow is such that mass, momentum, and energy are conserved across a shock, K is given by Eq. (5) or in terms of M_1^2 by

$$K = \frac{2\gamma M_1^2 - (\gamma-1)}{\gamma+1}\left[\frac{(\gamma-1)M_1^2+2}{(\gamma+1)M_1^2}\right]^\gamma \tag{14}$$

and Eq. (13) reduces to Eq. (3). In other words, by a nonisentropic formulation with the entropy given by Eq. (14), the Rankine-Hugoniot shock strengths are obtained. The momentum deficit vanishes for this nonisentropic formulation. It can be shown that if any two of the three conservation equations are satisfied and the entropy is as given by Eq. (14), then the Rankine-Hugoniot shock jumps are obtained and, furthermore, the third conservation equation is also satisfied. Thus, it is possible with this nonisentropic potential formulation to obtain both the mathematical convenience by the proper choice of the two conservation equations and physical accuracy by specifying the entropy according to Eq. (14).

There is, of course, some additional work required to implement the nonisentropic potential formulation. During the course of a numerical solution, for example, the shock wave location, the entropy field, and the streamline locations (for a two-dimensional flow) must be either known or computed. The first requirement is not very restrictive, since most numerical codes use a type of dependent algorithm that switches at the shock wave, thus allowing easy identification of the shock locations. The accuracy of the remaining two requirements will be discussed in the next section. Also covered will be the connection between the entropy and vorticity through Crocco's theorem.[1,2]

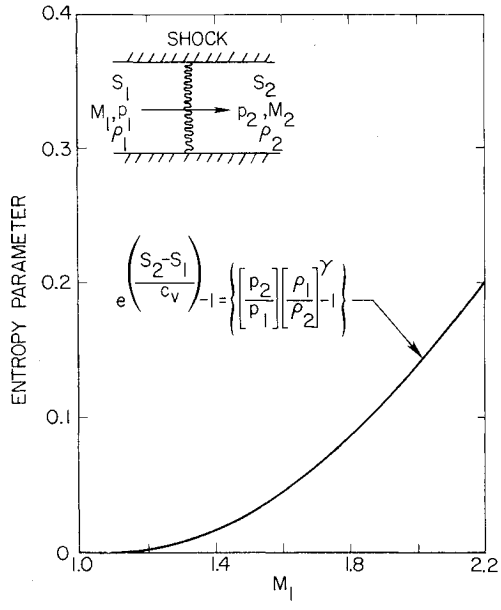

Fig. 3 Entropy rise through a one-dimensional Rankine-Hugoniot shock wave.

In some ways, this formulation is more convenient than solving the conservation equations of mass, momentum, and energy. Since the conservation equation for mass can be replaced by a stream function and it can be shown that the entropy is constant along a streamline, the problem can be also solved for the stream function, the vorticity, and the entropy. Such a solution procedure has been developed by Hafez and Lovell.[10]

In solving for the stream function in a transonic flow, there is a problem with the double-valued density/velocity relation at the sonic point since the solution must change solution branches. Furthermore, in three dimensions two stream functions are necessary to model the flow, which complicates the problem, and in unsteady flow a stream function cannot be defined.

It is the aim of the present analysis to investigate whether a nonisentropic potential theory can be satisfactorily evolved, which retains the simplicity of the potential formulation but without the complications in three-dimensional or unsteady flows of the stream function formulation.

III. Small-Perturbation Expansion of Crocco's Theorem

In existing transonic potential flow computations for flows with shock waves, momentum is not conserved across the shock wave. In a more general potential formulation, which conserves any two of the conservation equations, there will be an error in the third conservation quantity. Hence, in this section, Crocco's theorem will be rederived from the Euler equations with arbitrary conservation errors, Gibb's relation, and a vector identity. A similar analysis is presented in Ref. 4 for the traditional potential equations. Crocco's theorem[1,2] provides the relation between irrotationality and isentropy used in the traditional potential approximations in transonic flows. However, Crocco's theorem relates the entropy and conservation error gradients to vorticity and thus the assumption of isentropy may be unnecessarily restrictive.

The steady Euler equations in strongly conservative form with arbitrary conservation errors are

mass:

$$\nabla \cdot \{\rho q(1+\epsilon_\rho)\} = 0 \tag{15}$$

momentum:

$$\nabla\cdot\{\rho qq\}+\nabla\{p(1+\epsilon_m)\}=0 \tag{16}$$

energy:

$$\nabla\cdot\{h_0\rho q(1+\epsilon_e)\}=0 \tag{17}$$

The conservation errors of the mass, momentum, and energy equation are ϵ_ρ, ϵ_m, and ϵ_e, respectively. By expanding the energy equation into nonconservative form and using the continuity equation, one obtains

$$\rho q\cdot\nabla\left(h_0\frac{1+\epsilon_e}{1+\epsilon_\rho}\right)=0 \tag{18}$$

This states that instead of total enthalpy being constant along a streamline, the quantity

$$h_0\left(\frac{1+\epsilon_e}{1+\epsilon_\rho}\right)$$

is now constant. Assuming uniform reservoir conditions with $\epsilon_{e\infty}=\epsilon_{\rho\infty}=0$, one obtains

$$h_0\left(\frac{1+\epsilon_e}{1+\epsilon_\rho}\right)=h_{0\infty} \tag{19}$$

everywhere. It can be seen that the constancy of total enthalpy is modified by the conservation errors of both the continuity and energy equations.

Crocco's theorem is derived from the conservation equations of mass, momentum, and energy, Gibbs relation

$$T\nabla S=\nabla h-(1/\rho)\nabla p \tag{20}$$

and the vector identity

$$(q\cdot\nabla)q=\nabla\frac{q^2}{2}-q\times\mathrm{curl}q \tag{21}$$

It is given by

$$T\nabla S+q\times\mathrm{curl}q$$
$$=\frac{1}{\rho}[\nabla(\epsilon_m p)-q\nabla\cdot(\rho q\epsilon_\rho)]+h_{0\infty}\nabla\left(\frac{1+\epsilon_\rho}{1+\epsilon_e}\right) \tag{22}$$

where use has been made of Eq. (19).

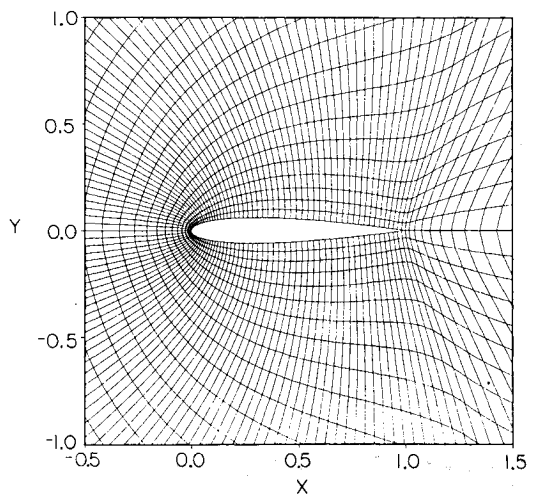

Fig. 4 Grid plot of a C mesh around a NACA 0012 airfoil (175×31 mesh points).

This form of Crocco's theorem reveals that the relation between entropy and vorticity is modified by the conservation errors. Unless the gradients of the conservation errors vanish, the usual equivalence of irrotational and isentropic flow is no longer true. Equation (22) shows that the basic assumptions of the traditional potential formulation are not valid. As was shown in the previous section for the traditional formulation, $\nabla S=0$, $\epsilon_\rho=\epsilon_e=0$, and $\epsilon_m\neq 0$. Therefore, in general $\nabla(\epsilon_m p)\neq 0$ and thus $q\times\mathrm{curl}q\neq 0$. In other words, a potential does not exist. This is also true for the nonisentropic potential formulation where $\nabla S\neq 0$ and $\epsilon_\rho=\epsilon_e=\epsilon_m=0$.

In Cartesian coordinates in two dimensions, Eq. (22) becomes, with slight rearrangement

$$(1+\epsilon_m)\frac{p}{\rho}\frac{\partial}{\partial x}\left(\frac{S}{R}\right)=-v\left(\frac{\partial v}{\partial x}-\frac{\partial u}{\partial y}\right)+h_{0\infty}\frac{\partial}{\partial x}\left(\frac{1+\epsilon_\rho}{1+\epsilon_e}\right)$$
$$+\frac{p}{\rho}\frac{\partial}{\partial x}\epsilon_m-u\left[u\frac{\partial}{\partial x}\ell n(1+\epsilon_\rho)+v\frac{\partial}{\partial y}\ell n(1+\epsilon_\rho)\right]$$
$$+\frac{\gamma}{\gamma-1}\frac{p_\infty}{\rho_\infty}\left(1+\frac{\gamma-1}{2}M_\infty^2\right)\epsilon_m\frac{\partial}{\partial x}\xi \tag{23}$$

and

$$(1+\epsilon_m)\frac{p}{\rho}\frac{\partial}{\partial y}\left(\frac{S}{R}\right)=u\left(\frac{\partial v}{\partial x}-\frac{\partial u}{\partial y}\right)+h_{0\infty}\frac{\partial}{\partial y}\left(\frac{1+\epsilon_\rho}{1+\epsilon_e}\right)$$
$$+\frac{p}{\rho}\frac{\partial}{\partial y}\epsilon_m-v\left[u\frac{\partial}{\partial x}\ell n(1+\epsilon_\rho)+v\frac{\partial}{\partial y}\ell n(1+\epsilon_\rho)\right]$$
$$+\frac{\gamma}{\gamma-1}\frac{p_\infty}{\rho_\infty}\left(1+\frac{\gamma-1}{2}M_\infty^2\right)\epsilon_m\frac{\partial}{\partial y}\xi \tag{24}$$

where

$$\xi=\left(\frac{1+\epsilon_\rho}{1+\epsilon_e}-\frac{\gamma-1}{\gamma+1}\frac{q^2}{a^{*2}}\right)$$
$$\frac{p}{\rho}=\frac{p_\infty}{\rho_\infty}\left(1+\frac{\gamma-1}{2}M_\infty^2\right)\xi \tag{25}$$

and

$$\frac{p}{p_\infty}=\left(\frac{\rho}{\rho_\infty}\right)^\gamma\exp\left[\frac{s-s_\infty}{c_v}\right] \tag{26}$$

By use of Eq. (25), the right-hand sides of Eqs. (23) and (24) are in terms of the velocities and the conservation errors only.

Expanding the right-hand sides of eqs. (23) and (24) in terms of perturbation velocities $\bar{u}$ and $\bar{v}$

$$u=q_\infty(1+\bar{u}),\qquad v=q_\infty\bar{v}$$

and retaining only the lowest-order terms leads to the following small-perturbation expansion of Crocco's theorem:

$$\theta\frac{\partial}{\partial x}\left(\frac{S}{R}\right)=\lambda\frac{\partial}{\partial x}(\epsilon_\rho-\epsilon_e)+\frac{\partial}{\partial x}\epsilon_m \tag{27}$$

and

$$\theta\frac{\partial}{\partial y}\left(\frac{S}{R}\right)=\gamma M_\infty^2\left(\frac{\partial\bar{v}}{\partial x}-\frac{\partial\bar{u}}{\partial y}\right)+\lambda\frac{\partial}{\partial y}(\epsilon_\rho-\epsilon_e)+\frac{\partial}{\partial y}\epsilon_m \tag{28}$$

where

$$\theta=(1+\epsilon_m)\frac{p}{p_\infty}\frac{\rho_\infty}{\rho}$$

and

$$\lambda=\frac{\gamma}{\gamma-1}\left(1-\frac{\gamma-1}{2}M_\infty^2\right)$$

Note that the conservation errors are of the $0(\tilde{u}^3)$ as can be shown from the momentum deficit, for example, since

$$\epsilon_m=\frac{\Delta(\rho u^2+p)}{(\rho u^2+p)_1}\approx-\frac{2}{3}\left(\frac{1}{\gamma+1}\right)^3(M_1^2-1)^3\approx(\tilde{u}_1-\tilde{u}_2)^3$$

For steady flows it can be shown that the entropy and conservation errors are constant along streamlines except at the shock waves. Therefore, the streamwise (x direction) gradients of entropy and conservation errors vanish in the regions of continuous flows and thus Eq. (27) is identically satisfied. To the lowest order, the vorticity $[(\partial\tilde{v}/\partial x)-(\partial\tilde{u}/\partial y)]$ appears only in the second of Eqs. (27) and (28) and therefore depends solely on the normal y gradients of entropy and conservation errors. In general, the normal gradients do not vanish except for shock jumps of zero or constant strength. We have shown in the previous section that the entropy changes or conservation errors cannot be simultaneously zero. Therefore, the vorticity generation can never vanish for flows with curved discontinuities, even if the flow is considered to be isentropic across the shock wave. The conservation errors or the entropy changes across a shock are of $0(\tilde{u}^3)$. Thus, the vorticity produced at a curved shock is of $0(\tilde{u}^3)$.

Since it has been shown that a flow with curved discontinuities can never be irrotational and thus the traditional potential formulation is inconsistent, it seems reasonable to expect that a nonisentropic potential formulation (also inconsistent) can resolve the shock waves better.

IV. Nonisentropic Potential Equation

The derivation of the nonisentropic potential equation is similar to that given in Ref. 5, the major difference being the inclusion of the entropy changes. In this formulation the conservation equations are satisfied exactly, so there are no conservation errors for the one-dimensional case.

In dimensional form the energy equation is

$$\frac{\gamma\tilde{p}}{(\gamma-1)\tilde{\rho}}+\frac{\tilde{q}^2}{2}=\frac{\gamma\tilde{p}_0}{(\gamma-1)\tilde{\rho}_0}=\frac{\tilde{a}^{*2}}{\gamma-1}+\frac{\tilde{q}^{*2}}{2}=\frac{\tilde{a}^{*2}}{2}\left(\frac{\gamma+1}{\gamma-1}\right) \quad (29)$$

where $(\tilde{\ })$ denotes dimensional quantities. Normalizing with a^* and ρ_0 (critical sound speed and stagnation conditions) obtains

$$\frac{2\gamma}{\gamma+1}\frac{p}{\rho}+\frac{\gamma-1}{\gamma+1}q^2=1 \quad (30)$$

From the Gibbs relation and perfect gas with constant c_v and c_p, we obtain

$$p=\frac{\gamma+1}{2\gamma}K\rho^\gamma \quad (31)$$

where

$$K=\exp[(s-s_0)/c_v] \quad (32)$$

Substituting into the energy equation obtains

$$\rho=\left[K^{-1}\left(1-\frac{\gamma-1}{\gamma+1}q^2\right)\right]^{1/(\gamma-1)} \quad (33)$$

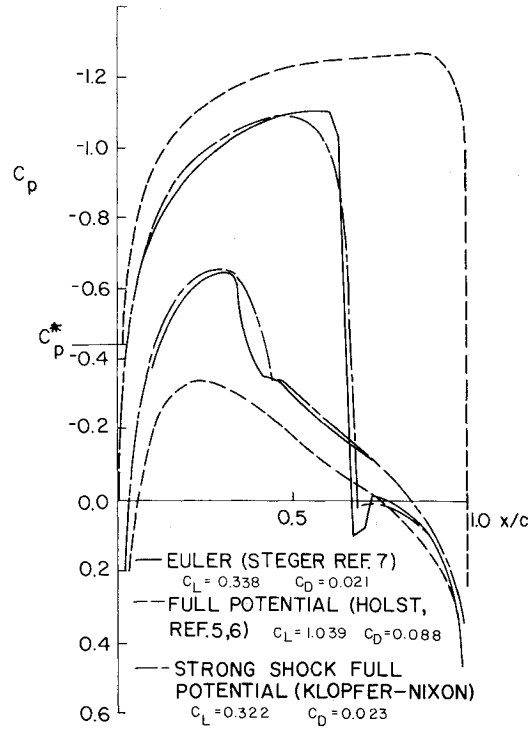

Fig. 5 Pressure distribution around a NACA 0012 airfoil at $M_\infty=0.80$ and $\alpha=1.25$ deg.

from which the Mach number is

$$M^2=\frac{q^2}{a^2}=\frac{2}{\gamma-1}\left(\frac{1}{K}\rho^{1-\gamma}-1\right) \quad (34)$$

The steady flow continuity equation in two dimensions is

$$(\rho u)_x+(\rho v)_y=0 \quad (35)$$

Assuming that shock waves are nearly normal to the u velocity vector, then we need to consider only the one-dimensional case to arrive at the proper jump relations. The jump relations for the one-dimensional steady Euler equation reduce to $\tilde{u}_1\tilde{u}_2=a^{*2}$. With the above normalizations this becomes

$$u_1u_2=1 \quad (36)$$

This equation is also known as Prandtl's relation. The jump relations for the potential equation are

$$\rho_1u_1=\rho_2u_2$$

and from Eq. (33)

$$\left[\frac{1-[(\gamma-1)/(\gamma+1)]u_1^2}{K_1}\right]^{1/(\gamma-1)}u_1=\left[\frac{1-[(\gamma-1)/(\gamma+1)]u_2^2}{K_2}\right]^{1/(\gamma-1)}u_2 \quad (37)$$

Solving for K_2/K_1, substituting for $u_2=1/u_1$, and setting $K_1=1$ and $K_2=K$ results in

$$K=\frac{u_1^2-[(\gamma-1)/(\gamma+1)]}{1-[(\gamma-1)/(\gamma+1)]u_1^2}\left(\frac{1}{u_1^2}\right)^\gamma \quad (38)$$

Equation (38) is the same as Eq. (14), except for the differences between u_1 and M_1. The relation between the two is

$$u_1^2 = \frac{(\gamma+1)M_1^2}{2+(\gamma-1)M_1^2} \tag{39}$$

Thus, the only modification required for a standard potential formulation such as given in Ref. 5 is that the shock location and upstream velocity is required, K is computed from Eq. (38), the density and pressure are given by Eqs. (33) and (31), respectively, and the local Mach number by Eq. (34). Since the entropy (or K) is a particle property, it is constant along the streamlines and changes only through the shock waves by Eq. (38). Therefore, the streamline locations need to be known. This can be done iteratively, but in the present work it is assumed that a rough estimate is sufficient for most nonseparated external transonic flows and the use of a C-type mesh, where the mesh conforms to the wing surface and wake, is probably adequate. The reason for this is that the streamline at the airfoil surface coincides with the surface and is then known. It is at this location that the greatest effect of entropy is felt.

The final modification required to implement the nonisentropic formulation involves the Kutta condition on the trailing edge of the airfoil. In the isentropic formulation, the far-field circulation is the same as the circulation around the airfoil, since the circulation around the wake alone is zero. The airfoil circulation is given by the potential jump across the edge of the airfoil. However, for a nonisentropic formulation, since the pressure as given by Eq. (31) determines the proper Kutta condition, i.e., no transverse pressure gradient at the trailing edge, the wake circulation is in general nonzero because of the jump in K on the wake bounding streamline gives a different p-ρ relation. The far-field circulation is now no longer simply related to the potential jump at the trailing edge. It must be deduced from the airfoil and wake circulation. In this paper, the far-field circulation is set so that the pressure jump across the wake at the trailing edge is zero. The wake position is fixed along the x-coordinate axis, see Fig. 4. The pressure jump across the wake vanishes if the potential along the upper side of the wake is given by

$$\phi_{\text{upper}}(x) = \phi_{\text{lower}}(x) + \phi_{\text{upper}}(x=1) - \phi_{\text{lower}}(x=1) + (x-1)\beta(S)$$

where $x=1$ denotes the trailing edge of the airfoil and β a function of the entropy jump across the wake.

In the above derivation, we have assumed that the shock waves are nearly normal to the u velocity vector. However, the present formulation can, in principle, be easily generalized to include oblique shock waves in both two- and three-dimensional flows.

V. Numerical Results

The nonisentropic potential formulation was tested with some numerical computations. A standard potential code[5,6] modified for a C-type mesh was used. The changes as outlined in the previous section were implemented and tested for a NACA 0012 airfoil at several freestream Mach numbers and angles of attack.

The meshes for all cases are identical and consist of 175 points along the wake/airfoil direction and 31 points in a near normal direction to the wake/airfoil (see Fig. 4). The far-field boundary is about six chord lengths from the airfoil in all directions.

The results of the first case ($M_\infty = 0.8$, $\alpha = 1.25$ deg) are shown in Fig. 5 in terms of the pressure distributions on the airfoil surface. This example is an extreme case in that the full potential results give upper surface shock waves near the trailing edge of the airfoil, whereas the Euler results obtained with the code described in Refs. 7 and 8 locate the shock wave at about 60-70% of the chord. The strong shock (nonisentropic) potential formulation results are virtually identical to the Euler results. The location of the upper surface shock wave falls within the scatter of the various Euler solutions presented in Ref. 9. The strong shock potential equations also yield the lower surface shock wave predicted by the Euler equations. This lower surface shock wave is nonexistent in the full potential result. The differences that do exist between the Euler and strong shock potential equations may be due to the assumption of irrotationality for the latter equations.

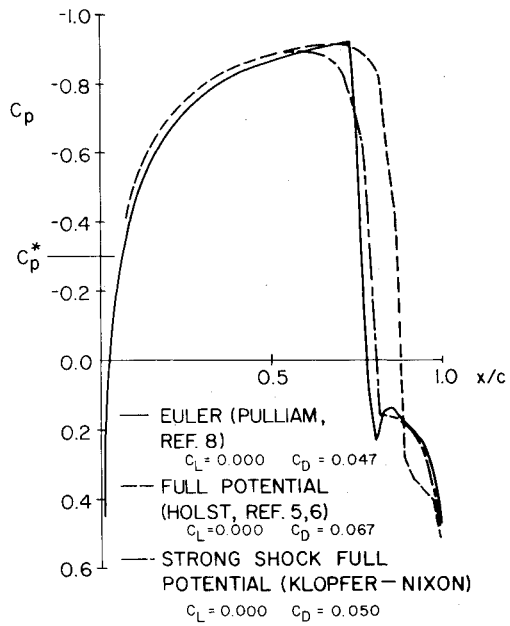

Fig. 6 Pressure distribution around a NACA 0012 airfoil at $M_\infty = 0.85$ and $\alpha = 0$ deg.

The improved results of the strong shock equation over the full potential equation is also reflected in the lift and drag coefficients shown in Fig. 5. The full potential lift is off by almost 300%, whereas the strong shock potential lift is off by less than 5% from the Euler results. The drag coefficients indicate a similar improvement, although the numerical calculations are not accurate enough to provide reliable drag results.

The above example is an unusual case in that the differences between the Euler and full potential results are quite large. Thus, this example is a good test case for the strong shock potential equation. The fact that the present nonisentropic potential formulation gives essentially Eulerian results seems to indicate that the neglect of entropy is the major cause of the difference between the Euler and full potential results. The vorticity seems to have very little, if any, effect for this case. It is known, however, that the full potential equations are associated with nonunique solutions, in which three solutions may be obtained for the same angle of attack and freestream Mach number.[9] The large differences shown by the above example may be due to the nonuniqueness problem and not necessarily to the neglect of entropy.

The second example is a nonlifting strong shock case ($M_\infty = 0.85$, $\alpha = 0$ deg). The nonuniqueness problem is avoided by forcing the far-field circulation to vanish for the potential results. These results are shown in Fig. 6. Again the strong shock results are very close to the Euler results. The lift is zero to four places as shown and the improvement in drag is apparent from the figure. This result clearly shows the important influence of the entropy as opposed to the vorticity for transonic flows.

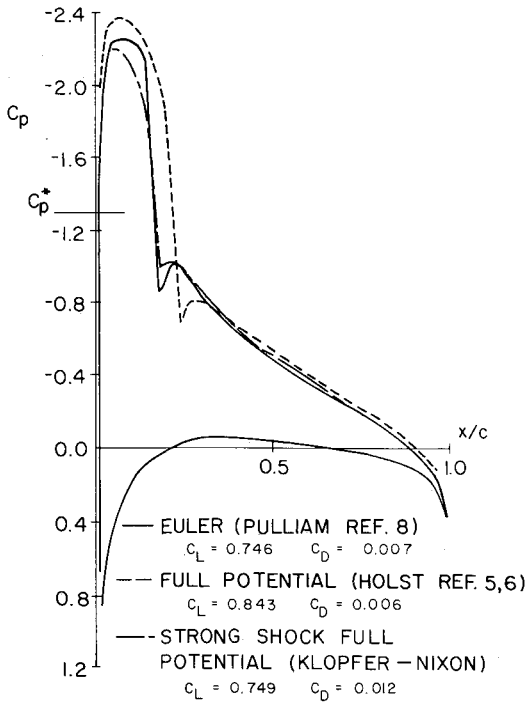

Fig. 7 Pressure distribution around a NACA 0012 airfoil at $M_\infty = 0.60$ and $\alpha = 5$ deg.

The third example is a lifting strong shock case with a very small supersonic bubble on the nose of the airfoil ($M_\infty = 0.6$, $\alpha = 5$ deg). Since the supersonic bubble is small and the shock is strong (preshock Mach numbers ≈ 1.4), the entropy gradients and thus the vorticity behind the shock is larger than for the previous two cases. Thus, it might be expected that the present strong shock formulation should fail for this case. However, as shown in Fig. 7 the difference between the Euler and strong shock results is small. The lift and shock location are virtually identical. The drag results are not reliable due to insufficient numerical accuracy. Even for this case where the vorticity might be expected to be important, it has been shown that the entropy is the dominating influence for transonic flows with shock waves. Thus, the present strong shock formulation gives essentially Eulerian results.

It may be possible that the strong shock potential equation avoids the nonuniqueness problem that occurs with the full potential equation. The reason for this is that the Euler results have (so far) not shown any of the nonunique solutions given by the full potential approximations. Since the present formulation gives essentially Eulerian results it is probable that it also will show only unique solutions.

VI. Conclusions

In this study the basic assumptions underlying the potential formulation of the Euler equations are examined. It is shown that the isentropic assumption is not necessary for the existence of a potential. It is also shown that the equivalence of isentropic flow and irrotational flow is false if any one of the conservation equations is violated.

By allowing the entropy changes and assuming irrotational flow a potential approximation to the the Euler equations is formulated. Some numerical calculations of the flowfields about a NACA 0012 airfoil indicate that the present theory yields results that are nearly indistinguishable from those of the Euler code. The computation time is only a fraction (10%) of the CPU time required for the Euler results.

Acknowledgments

Research sponsored by the Air Force Office of Scientific Research under Contract F49620-79-C-0054. The United States Government is authorized to reproduce and distribute reprints for government papers not withstanding any copyright notation hereon.

References

[1]Crocco, L., "Eine neue Stromfunktion fur die Erforschung der Bewegung der Gase mit Rotation," *Zeitschrift fuer Angewandte Mathematik und Mechanik*, Vol. 17, No. 1, Feb. 1937, pp. 1-7.

[2]Vazsonyi, A., "On Rotational Gas Flows," *Quarterly of Applied Mathematics*, Vol. E, No. 1, April 1945, pp. 29-37.

[3]Murman, E. M., Yoshihara, H., and Korn, D., "Transonic Aerodynamics Notebook," *AIAA Short Course Series*, AIAA, New York, 1974.

[4]Nixon, D. and Klopfer, G. H., "Some Remarks on Transonic Potential Theory," *Journal of Applied Mechanics*, Vol. 50, No. 2, June 1983, pp. 270-274.

[5]Holst, T. L., "An Implicit Algorithm for the Conservation Transonic Full Potential Equation Using an Arbitrary Mesh," *AIAA Journal*, Vol. 17, Oct. 1979, pp. 1038-1056.

[6]Dougherty, F. C., Holst, T. L., Gundy, K. L., and Thomas, S. D., "TAIR—A Transonic Airfoil Analysis Computer Code," NASA TM 81296, May 1981.

[7]Steger, J. L., "Implicit Finite Difference Simulation of Flow About Two-Dimensional Geometries," *AIAA Journal*, Vol. 16, July 1978, pp. 679-686.

[8]Pulliam, T. H., Jespersen, D. C., and Childs, R. E., "An Enhanced Version of an Implicit Code for the Euler Equations," AIAA Paper 83-0344, Jan. 1983.

[9]Rizzi, A. and Viviand, H. (eds.), "Numerical Methods for the Computation of Inviscid Transonic Flows with Shock Waves," *Notes on Numerical Fluid Mechanics*, Vol. 3, GAMM Workshop, Vieweg, 1981.

[10]Hafez, H. and Lovell, D., "Numerical Solution of Transonic Stream Function Equation," AIAA Paper 81-1017, June 1981.